Excited state charge separation in symmetrical alkenes

Zijlstra, Robert Wiebo Johan

Solvent Dependent Excited State Dynamics and Charge Separation of *Para*-Substituted TPEs

6.1 Introduction

As reported in the introduction of the previous chapter, tetraphenylethylene (TPE) has been widely used as a model alkene in a large number of spectroscopical investigations with the aim to study the sudden polarization effect in the condensed phase[1-11]. In these investigations, the solvent dependent TPE excited state lifetimes and dynamics as well as its electronic nature have been studied by various techniques. It has been established that a polar form (i.e. a CT state) of the twisted TPE excited state does exist,[3-7, 9, 11] even though evidence has been provided that this is not the only state present at this geometry, especially in nonpolar solvents. These findings have been confirmed by the femtosecond pump-probe measurements presented in the previous chapter, where a dramatic difference in the TPE excited state lifetime and absorption spectrum was observed between polar and nonpolar solvents. Especially an absorption band around 500 nm, which was intense in polar solvents only and which was formed after several picoseconds, could be assigned to the twisted CT state of TPE. However, the much weaker intensity of this absorption in cyclohexane strongly suggested a less populated CT state in this medium. This was confirmed by fitting the various data sets to a kinetic model, which revealed the existence of another twisted excited state in cyclohexane. This second twisted excited state was assumed to be non-absorbing at 500 nm and of a nonpolar nature.

The main reason for the (D_2-symmetrical) TPE being the popular choice in the aforementioned studies is the fact that, apart from it meeting the symmetry requirements to study the sudden polarization effect, TPE is a commercially available compound which is soluble in a large number of organic solvents. Unsurprisingly, much less is known about the impact of the addition of substituents to the TPE phenyl rings on both the twisting dynamics and the charge separation process, not in the least because such compounds are not as readily available as TPE itself. This is unfortunate, since the availability of such information could provide valuable insights on, for instance, the tunability of the CT states in symmetrical alkenes by means of the introduction of electron directing substituents at the phenyl rings.

Only a few studies have been reported on *para*-substituted TPE's[4, 6, 9] (figure 6.1). First of all, Ma and Zimmt published a study[9] in which they investigated four different compounds (**I** to **IV**) by means of picosecond optical calorimetry in methylcyclohexane.

It was observed that for all compounds except for **II** an equilibrium exists between two conformationally relaxed states and that an intense long-lived fluorescence could be detected with an emission maximum at $\lambda = 542$ nm[4]. Between compounds **I**, **III** and **IV**, only small differences where observed even though **III** and **IV** showed a slight increase in both fluorescence quantum yield and excited state decay rate.

These observations did not apply to compound **II**, however, which barely showed any steady state fluorescence and had a much shorter excited state lifetime. This was explained by assuming more explicit CT nature for the excited state of **II**, which prevented recrossing to the other conformationally relaxed state held responsible for the observed fluorescence.

Albeit not unexpected, this latter finding is still intriguing, since the non-symmetrical substitution of the two halves of the molecule in the case of compound **II**

apparently provides the necessary (intramolecular) symmetry breaking which might very well be solely responsible for effectively polarizing the twisted excited states, without requiring an external symmetry lowering perturbation (i.e. a solvent shell). This observation is a clear indication that minor modifications to the molecule structure already can have a dramatic effect on the CT behaviour of such compounds.

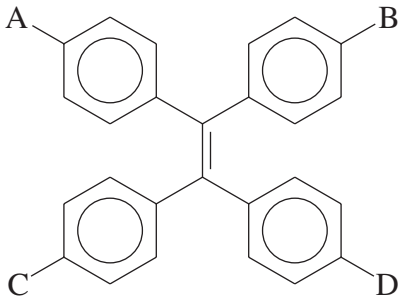

Figure 6.1

I A-D = H;
II A, B = H, C, D = CH_3;
III A≠B = (H, CH_3), C = H, D = CH_3;
IV A-D = CH_3

Another investigation involving a *p*-substituted TPE has been reported by Schuddeboom et al.[6] In this work, *para*-methoxy-TPE (A=B=C=D=OCH_3 in figure 6.1) as well as TPE itself have been studied by means of time-resolved microwave conductivity studies using cyclohexane and benzene as a solvent. It was established that the conformationally relaxed excited states of both TPE as well as its *p*-methoxy-subsituted analogue exhibited zwitterionic behaviour in cyclohexane. The nanosecond timescale of the experiments prohibited the detection of such behaviour in benzene, which is likely to be indicative of a shorter excited state lifetime in that particular solvent.

It is obvious that on the basis of the limited amount of information present no definite conclusions can be drawn regarding the role of the substituents on the TPE excited state behaviour, and that additional investigations are required. In order to gain more insight in the possible role of substituents on the TPE excited state shape and dynamics, this chapter will be dedicated to the investigation of a number of *p*-substituted TPE's by means of time resolved dual colour pump probe spectroscopy as described in chapter 5. The *p*-substituted TPE's presented in this chapter have been synthesized and characterized by means of ^{13}C NMR by Anne-Marie Schoevaars, for which she is gratefully acknowledged.

In the pump-probe experiments, the same experimental setup as described in chapter 5 has been used with one important modification. In the experiments reported in this chapter, the relative pump and probe beam polarizations have been oriented under a 45° angle with respect to each other. With a polarizing beam splitter, both the parallel (∥) and perpendicular (⊥) oriented signals have been separated behind the sample and detected simultaneously with two photodiodes of identical type. This is an important improvement, since it provides additional information regarding orientation of transition

dipoles and rotational diffusion[12]; topics which could only be briefly addressed in the previous chapter due to the separate detection of these signals there.
The following compounds have been investigated and compared:

1 A-D = H (see chapter 5 for more elaborate data)
2 A-D = CH_3
3 A-D = OCH_3
4 A-D = F
5 A-D = NO_2

The motivation for the selection of these particular components is that their substituents both exhibit electron donating (**2**, **3**) as well as electron withdrawing (**4**, **5**) behaviour in terms of the Hammett equation[13]. In this chapter, the interesting question is treated whether it is possible to utilize such effects in the 'tuning' of the charge separation in the excited states of the functionalized TPE's.
The excited state dynamics of all compounds has been investigated in the nonpolar solvent cyclohexane and the polar solvent ethanol. The only exception is compound **5**, which proved to be almost insoluble in the former. Solubility problems also prohibited the investigation of phenyl- and amino-substituted TPE's.

The outline of this chapter will be very similar to that of the previous one: first the excited state behaviour in the first two picoseconds will be described, followed by the dynamics at a longer timescale (~50 ps). The latter transients will be fitted to the same kinetic model as described in chapter 5 in order to compare the various results.

6.2 Results and Discussion

6.2.1 The First Two Picoseconds

For compounds **2-4**, the excited state behaviour in the first two picoseconds closely resembles that of TPE itself. The transients recorded in cyclohexane of **2-4** are compared in figure 6.2. Compound **5** showed anomalous behaviour which will be discussed later.

As in the case of **1** (TPE), the pump probe response of **2-4** is largely solvent independent over the first 2 ps. In the 650 nm transients, the same vibrational coherence can be observed as reported for **1**, even though the oscillations are somewhat less pronounced here. The main reason for this difference in amplitude is that the 650 nm pump pulse in the experiments described here was somewhat longer (~80 ps) than in the case of the experiments reported in chapter 5 (~65 ps). This pulse broadening was caused by a slight modification in the alignment of the quartz prisms used for the wavelength selection in front of the sample. This adjustment was made to allow inclusion of the blue part (400-450 nm) of the continuum. This resulted in a slight increase of prism material in the probe beam, thus altering the (non-linearity of the) chirp of the continuum pulse. Even though this chirp was compensated for by adjusting the positioning of the grating pair, the slightly longer pulse widths at the red part of the spectrum could not be avoided.

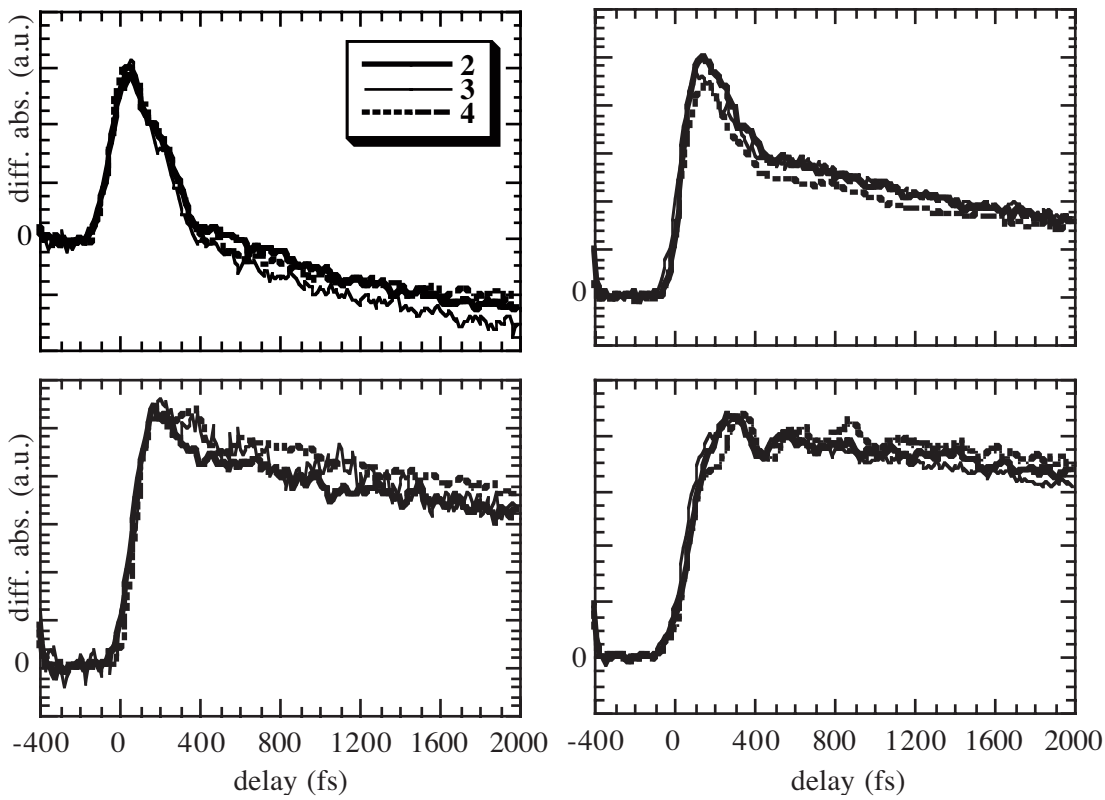

Figure 6.2 Pump probe spectra (|| polarization; difference absorption in arbitrary units) at 500 nm (top left), 550 nm (top right), 600 (bottom left) and 650 nm (bottom right plot) of the first 2 ps of **2**-**4** in cyclohexane.

It is apparent from figure 6.2 that the spectral evolution of **2**-**4** is quite similar in the first 2 ps.

However, some subtle differences can be observed when comparing them with **1**. This can be observed in figure 6.3, where the transients at 500 nm and 650 nm of **1** and **2** in cyclohexane are compared. The main difference is that the buildup of the stimulated emission at 500 nm as depicted in the top plot of figure 6.3 is somewhat slower in the case of the functionalized TPE's than in the case of TPE itself. Apparently the elongation of the C-C central bond, which in chapter 5 was held responsible for the large Stokes shift of this stimulated emission, appears to be somewhat delayed by the introduction of functional groups on the phenyl rings.

This is somewhat surprising especially in the case of **4**, since the small fluorine is only fractionally larger than a hydrogen atom[14] and much smaller than for instance a methyl group. The stimulated emission build-up rates of **2** and **4** are, however, comparable as can be seen from figure 6.2.

In figure 6.4 the pump-probe transient at 500 nm of tetrafluoroderivative **4** is compared to that of TPE itself. It appears that in the case of **1** and **4** the transients at 500 nm are more alike even though the build-up of the stimulated emission is still somewhat quicker (~ 50-100 fs). The most likely explanation for this small delay in the buildup of the stimulated emission in the case of **2**-**4** in comparison to **1** is that the C-C central bond elongation is accompanied by some initial twisting around this bond. The latter component of the dynamics can be responsible for the slower buildup, since it has been reported

before that the introduction of *p*-substituents on the phenyl rings introduces additional solvent drag, which slows down the twisting process[9]. These findings will be supported by the transient behaviour at longer time scales (*vide infra*).

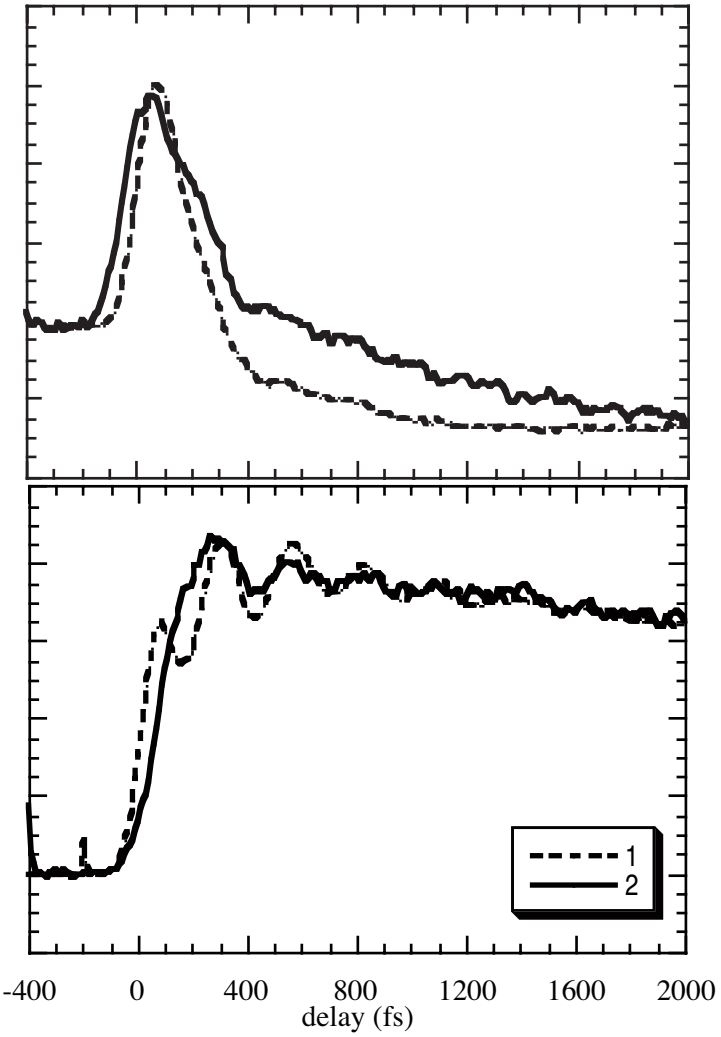

Figure 6.3 Pump probe spectra at 500 nm (top plot) and 650 nm (bottom plot) of the first 2 ps of **1** and **2** in cyclohexane.

Another observation that can be made from figure 6.3 is that the vibrational coherence observed at the 650 nm transient is more or less the same for both **1** and **2**, apart from amplitude of the beats and the behaviour in the first 100 fs. As already mentioned in chapter 5, the pulse shape of the 650 nm probe pulse has a distinct influence on the transient response[15] and the somewhat broader pulse used in the experiments reported here can be held responsible for the missing beat in the first 150 fs in the spectrum of **2**. Apart from that, the periodicity of the oscillations (124 cm^{-1}) is the same between **1** and **2.** These were attributed[10,11] to wavepacket dynamics in the scissoring motions of the geminal phenyl rings[16], which resembles the correlated motion of two interlocking ratchets. Apparently, these are unmodified for the *p*-substituted TPEs, which can be expected since the *p*-subtituents are situated on the axis of rotation of the phenyl

groups involved in these motions. This will drastically limit their influence on the rotation dynamics.

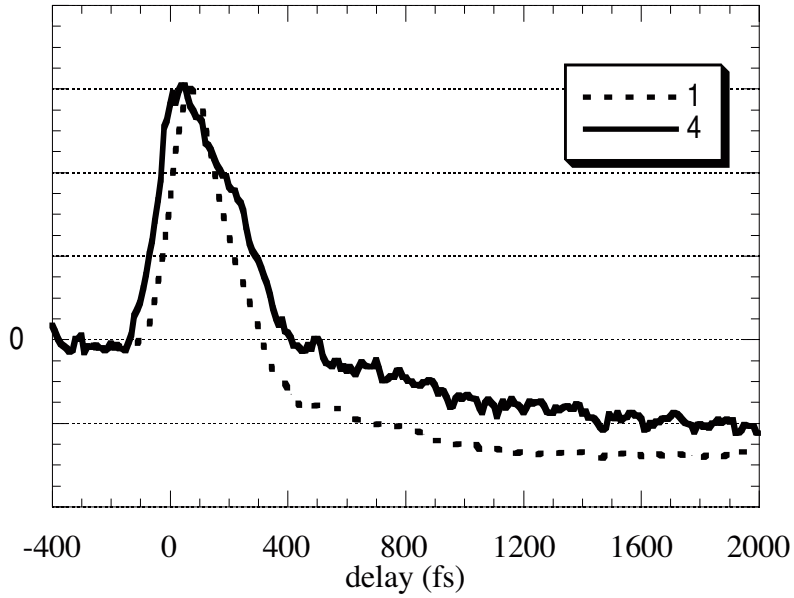

Figure 6.4 500 nm transients (|| orientation of pump and probe) of **1** and **4** in cyclohexane.

A validation of this assumption could be obtained by repeating these experiments with *o*- or *m*-substituted TPE's in which case the substituents are expected to have a more pronounced effect on the scissoring motions. This is beyond the scope of the present study though.

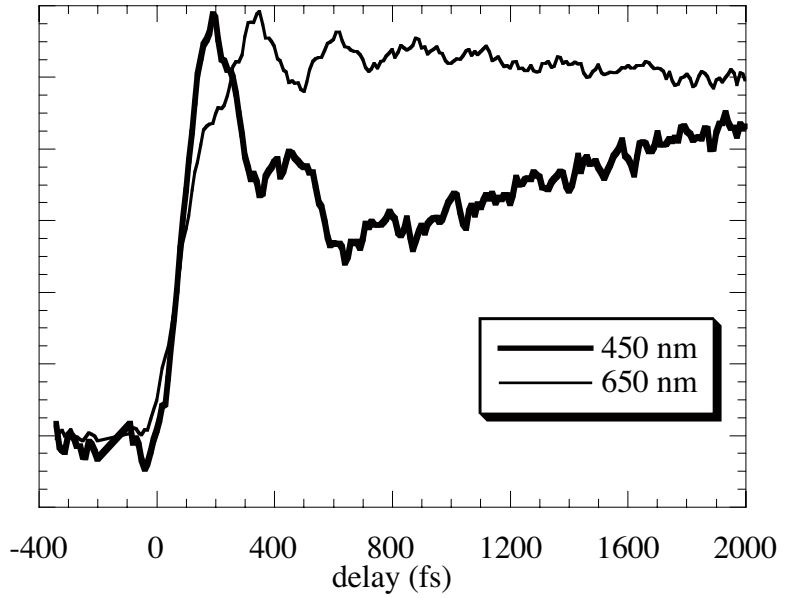

Figure 6.5 450 nm (bold line) and 650 nm (thin line) transients of **2** in cyclohexane (|| pump probe polarization orientation)

A highly relevant observation supporting the assignment of the oscillations to these scissoring motions is made in the absorption spectra of **2**-**4** at 450 nm (figure 6.5).
A complication of measuring at 450 nm is that the t=0 fs point, i.e. the point where pump and probe pulse coincide, could not be determined by the routine autocorrelation technique[12] due to the fact that the difference frequency of the pump and probe pulses lies well within the infrared part of the spectrum. At the time of these experiments, no appropriate detection was available. The t=0 point has been estimated by mapping the rising flank of the probe response at 450 nm on that of 650 nm.

Figure 6.5 clearly shows the 450 nm oscillations to be in almost perfect counterphase with that observed at 650 nm. As explained in the theoretical description in chapter 5 (see also figure 5.2), this is fully consistent with what one would expect for wave packet dynamics on a bound potential, where the transients at the inner and outer probe frequencies exhibit oscillations in counterphase with respect to each other[17-20]. Since this wavelength was not available on the original experimental setup used in the case of **1**, the oscillations at 450 nm were not detected in the experiments reported in chapter 5.

Finally, the excited state behaviour of **5** has to be discussed. Figure 6.6 shows the excited state behaviour of **5** probed at 650 nm. Quite surprisingly, within 500 fs the 650 nm transient transforms into a 'steady state' absorption lacking any significant decay dynamics, even after hundreds of picoseconds. The same behaviour is also observed at the other probe wavelengths. On the basis of the sub-nanosecond dynamics, it is estimated that the lifetime of **5** extends towards the μs domain, which is indicative of the existence of a triplet excited state. It is well documented that triplet states can be formed effectively in the presence of NO_2-groups[21-23]. Therefore, the most likely explanation for this phenomenon is that a rapid avoided crossing between the originally populated S_1 surface and a localized excitation on the NO_2 groups takes place, after which the observed triplet state is formed by highly efficient intersystem crossing. In conclusion, the excited state behaviour of **5** is completely different from that of the other TPE's and will therefore be excluded from further discussions.

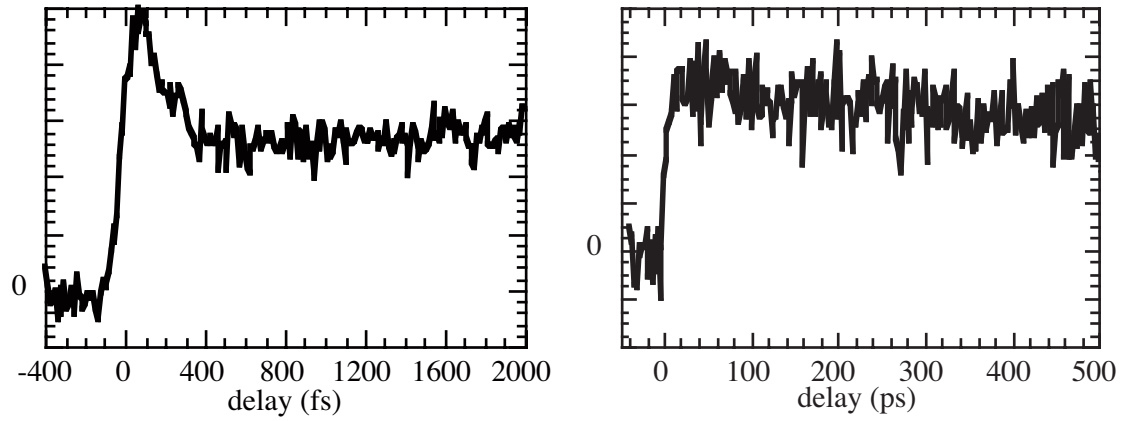

Figure 6.6 650 nm transients of **5** in ethanol. Left panel depicts the first 2 ps, right panel depicts the behaviour on sub-ns time scales.

6.2.2 Longer Time Scales in Cyclohexane

Figure 6.7 depicts the pump probe transients (‖ orientation) of **2**, **3** and **4** at longer time scales in cyclohexane. From figure 6.7 it becomes clear that all three compounds show roughly the same behaviour within the investigated timeframe, especially for the red part of the spectrum. At the green part some more substantial, albeit still minor, differences occur. Two observations can be made: first of all, the intensity of the stimulated emission of **4** appears to be weaker than that of **2** and **3**. Furthermore, **2** and **4** show a buildup of an absorption at 550 nm (similar to **1** in this solvent), which appears to be somewhat weaker for **3**.

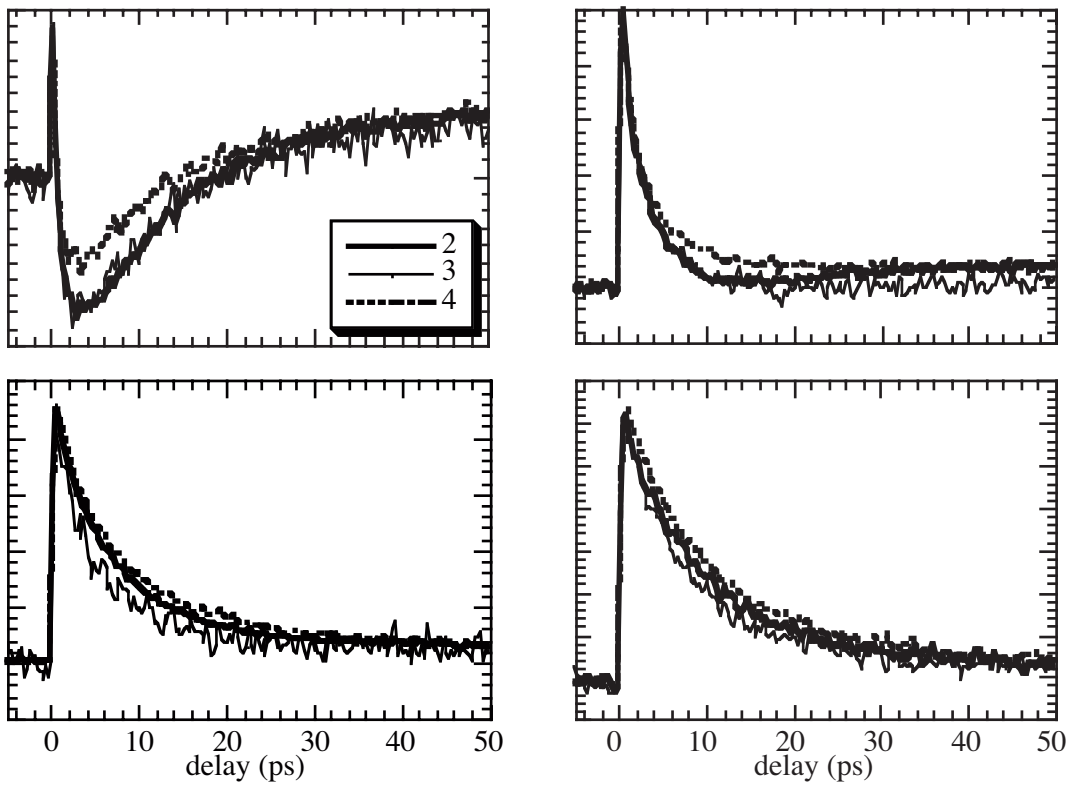

Figure 6.7 Pump probe spectra (‖ pump probe polarization orientation) up to 50 ps at 500 (top left), 550 (top right), 600 (bottom left) and 650 nm (bottom right panel) of **2**, **3** and **4** in cyclohexane.

At this stage, it becomes relevant to focus on the polarization dependent behaviour of the various transients[12]. Figure 6.8 shows the ‖ versus ⊥ polarization orientation of the 600 and 500 nm transients of **2**-**4** in cyclohexane. The data prove to be rather puzzling and difficult to interprete. First of all, the 600 nm transients show comparable behaviour for **2**-**4**, in which the depolarization of the transients occurs on a timescale of 10-20 ps. The 550 and 650 nm transients behave similarly. The depolarization rate of **3** is the highest (10 ps), followed by **2** and **4** (20 and 25 ps respectively). Since the rate of twisting dynamics for **2**-**4** appears to be roughly the same, another explanation has to be found for this difference in depolarization rates. It is likely that this is somehow connected to the freely

rotating out-of-plane local dipoles associated with the methoxy groups of **3**, a feature absent in compounds **2** and **4**.

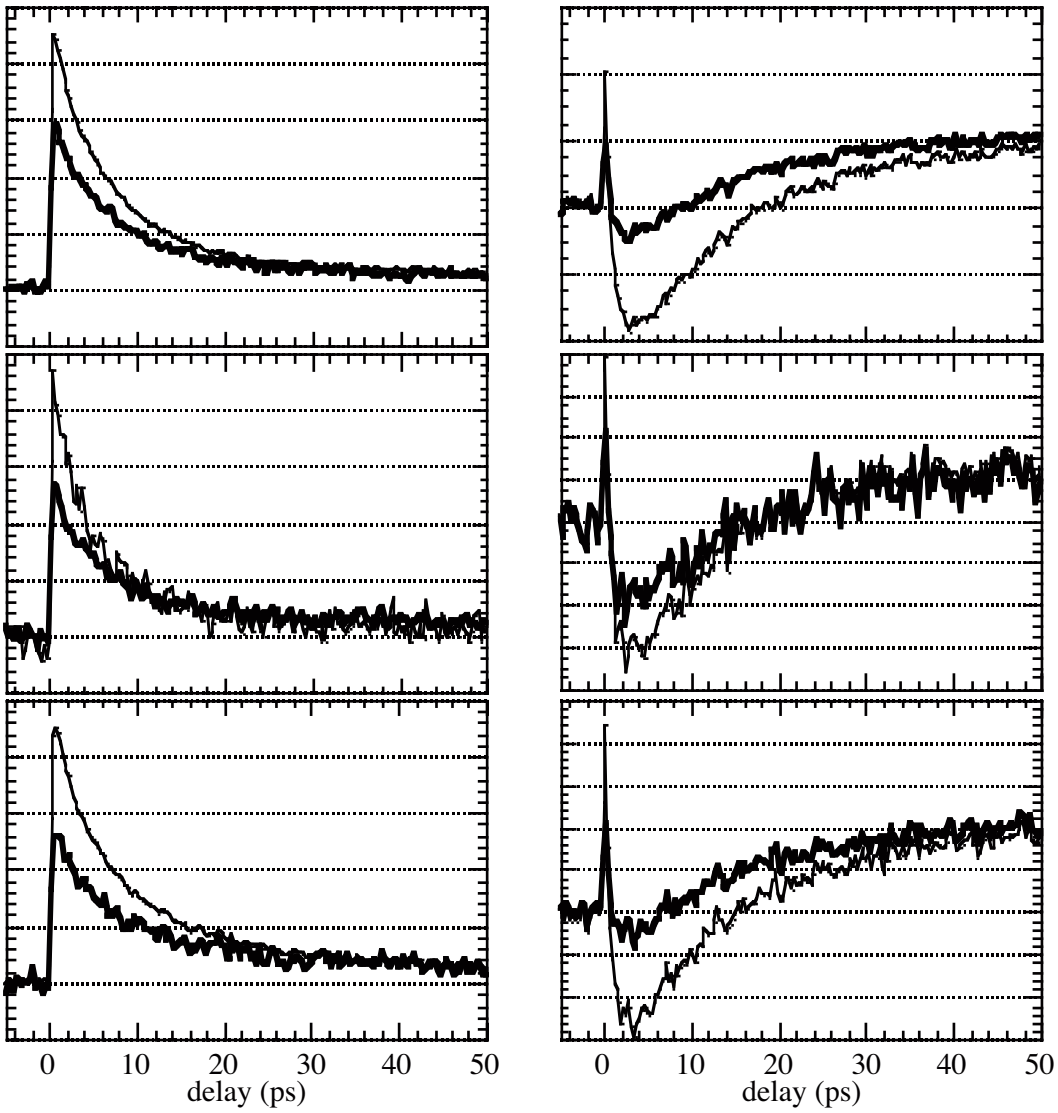

Figure 6.8 ∥ (thin line) and ⊥(bold line) pump probe orientations at 600 (left panels) and 500 nm (right panels) of **2**-**4** (from top to bottom) in cyclohexane.

When comparing the depolarization rates at the red part of the spectrum to the polarization dependent behaviour at 500 nm, it becomes clear that the rotational diffusion (i.e. the randomization of molecule orientation in the solvent) cannot be responsible for the observed decay in anisotropy. These transients show some complex behaviour. At first, when focussing on the lifetime of the stimulated emission occurring in the ∥ polarized spectrum at 500 nm, it appears to be roughly the same as the depolarization rates of the 600 nm transients. But at 20 ps, a substantial difference in transient intensity of the two polarization directions still exist in the case of **2** and **4**, and in fact this difference is still partly present at 50 ps in the case of **2**. This proves that the depolarization of the red part of the spectrum cannot be assigned to rotational diffusion, due to the fact that this would also cause complete depolarization at other wavelengths such as the 500 nm transients

examined here. Therefore, we have to conclude that two (or more) different modes of motion are being monitored. This can be explained in the following manner.

It has been reported before that the red part of the spectrum of the TPE excited state is connected to the twisting dynamics[1, 3, 11]. On the basis of this information and on the more intense absorption for the || oriented probe channel in the first picoseconds, it can be concluded that the orientation of the transition dipole moment with the probe at 600 nm is more or less parallel to that of the $S_1 \leftarrow S_0$ excitation, which exhibits a perpendicular orientation relative to the central double bond. The rotation of this bond randomizes the orientation of this transition dipole moment, which leads to the observed decay of the anisotropy at 600 nm. This can be regarded as an intramolecular reorganization which requires only a partial reorganization of the solvent cage.

The lifetime of the emission part of the spectrum at 500 nm is the same as that of the intramolecular rearrangement, responsible for the depolarization at the red part of the spectrum. This is another justification of the assumption that the observed transition at 600 nm has a transition dipole parallel to that of the $S_1 \leftarrow S_0$ transition as, for obvious reasons, the stimulated $S_0 \leftarrow S_1$ emission will also be polarized that way.

In addition, at 500 nm a second transition is probed. Due to the fact that this transition is more intense at the perpendicular pump probe orientation (see figure 6.8), it can be concluded that the transition dipole moment is oriented perpendicular to that of the $S_1 \leftarrow S_0$ excitation. Moreover, it appears to be unconnected to the central bond rotation, which must mean that the central bond rotation has no influence on the depolarization of this transition. Therefore, the orientation of the transition dipole moment of this excitation must be parallel to the axis of rotation of the central bond, hence (more or less) parallel to the central bond itself (figure 6.9).

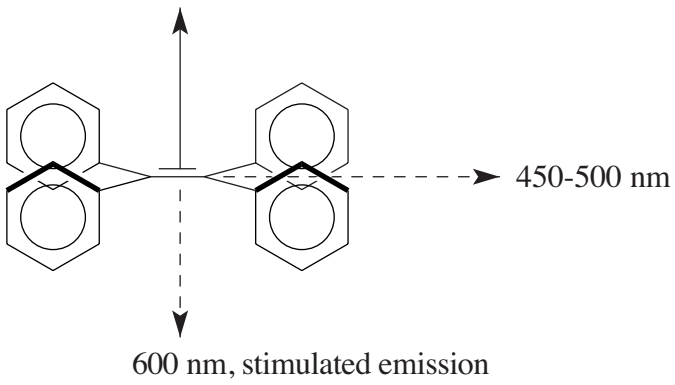

Figure 6.9 Schematic orientation of the proposed transition dipole moments of $S_1 \leftarrow S_0$ (solid arrow) and various $S_n \leftarrow S_1$ transitions (dashed arrows) of TPE. The 600 nm transition dipole is oriented anti-parallel to the $S_1 \leftarrow S_0$ transition for reasons of clarity only.

This picture is, of course, schematic and it is very well possible that the transition dipole of the 450-500 nm absorption will, for instance, be parallel to the C-C phenyl bond. But even then, central bond rotation will only partly depolarise the orientation of the

transition dipole moment and larger motions involving the whole molecule will have to take place to complete this process. Therefore, the complete depolarization of the 500 nm transient is ultimately caused by the (solvent dependent) rotational diffusion.

Confirmation for this theory can be found in the behaviour of the 450 nm transient. Figure 6.10 shows the 450 nm probe signal of **4** in cyclohexane. Intriguingly, at the perpendicular pump probe polarization, the absorption is immediately present upon excitation and the only dynamics observed are connected to the excited state lifetime of the molecule. For the parallel polarization however a buildup takes place which matches the perpendicular intensity at similar time scales as observed for the 500 nm transient. This is strong evidence for an orientation of the transition dipole moment perpendicularly to that of the $S_1 \leftarrow S_0$ for this particular excitation.

Additional evidence for the observation of two rather than one transition at 500 nm can be gained from analyzing the intensities of the ∥ and ⊥ channels (figure 6.8). For a probed transition with a transition dipole moment parallel to that of the initial excitation by the pump pulse, the intially observed ratio in the transient intensities of the two probe directions (∥ /⊥) should roughly be 3:1[12]. However, the stimulated emission at 500 nm, especially in the case of **2** and **4**, clearly exceeds this ratio. This can only be explained by assuming a simultaneous polarized absorption along the perpendicular channel which increases the aforementioned ratio. Compound **3** does not seem to exhibit this behaviour, the ratio observed in the stimulated emission between the respective probe orientations appears to be in accordance with a single transition with parallel transition moment. In addition, the complete depolarization of the 500 nm transient already takes place within 20 ps, much faster than in the case of **2** and **4**.

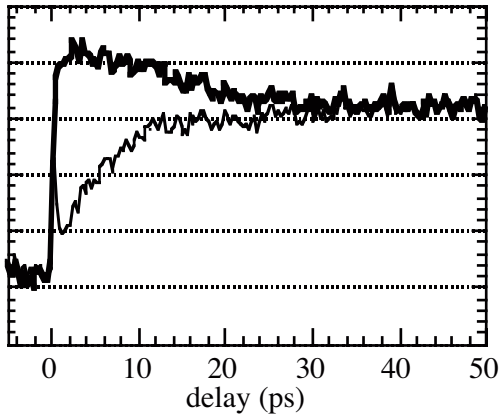

Figure 6.10 Pump probe spectrum (∥ thin line; ⊥ bold line) at 450 nm of **4** in cyclohexane.

There is a definite buildup of the 500 nm absorption in the spectrum of **3**, as was also observed for 2 and 4, but this absorption is already strongly depolarized over the first few picoseconds. Even though not yet fully understood, this must again be connected to the out-of-plane local dipole associated with the methoxy substituents of **3**. This considerable out-of-plane local dipole near the phenyl rings, which can shift quickly by the simple rotation of the C-O bond, is absent in **2** and **4**. If the fast randomization of the out-of-plane dipoles due to the rotation of the methoxy groups alters the direction of the

transition dipole of interest, this effect may be responsible for the rapid depolarization of the 500 nm probe signal of **3**. This depolarization decay then is not related at all to the rotational diffusion time of compound **3**.

6.2.3 Longer Time Scales in Ethanol

Next, the behaviour of **2**-**4** in ethanol will be analyzed. In figure 6.11 the pump probe spectra of **2**-**4** in ethanol are shown.Two remarkable observations were made. First of all, the behaviour at 500 nm is completely different for **2**, **3** and **4**. In the case of **1**, this absorption was assigned to its charge separated twisted excited state[11] (see also chapter 5), which would indicate significant differences in charge separation behaviour of **2**-**4**. This will be addressed in more detail later (*vide infra*).

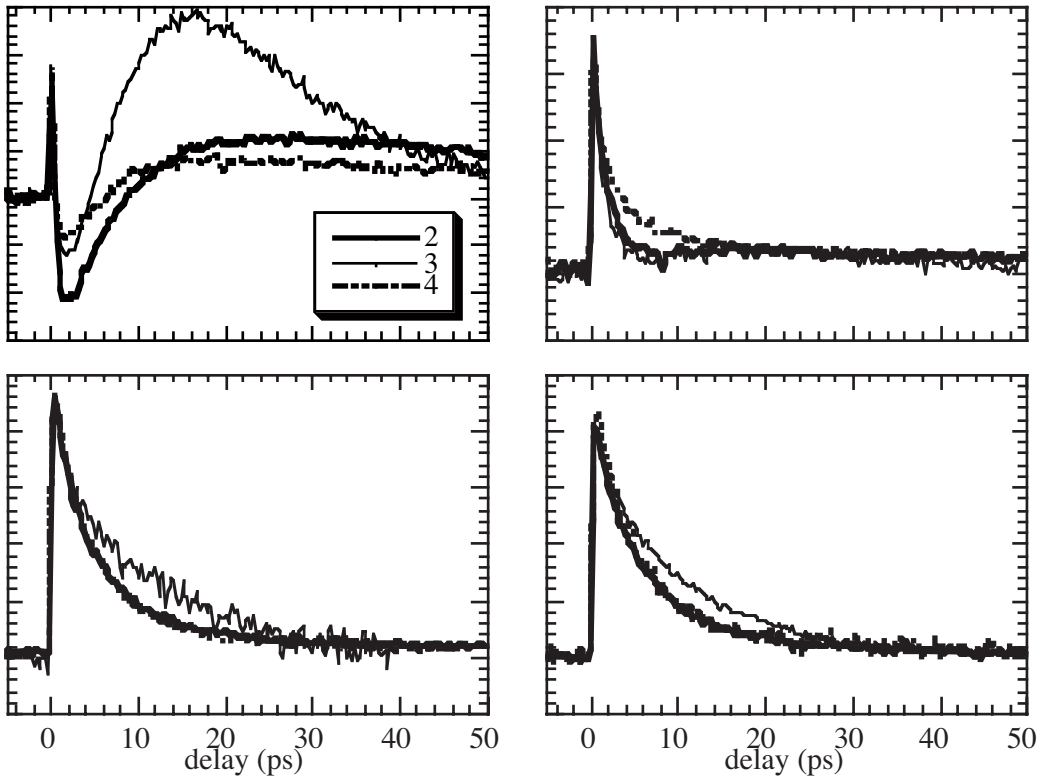

Figure 6.11 Pump probe spectra (|| pump probe orientation) at 500 (top left), 550 (top right), 600 (bottom left) and 650 nm (bottom right panel) of **2**-**4** in ethanol.

The second remarkable feature occurs in the red part of the spectrum. In contrast to the situation in cyclohexane (see figure 6.7), the central bond twisting dynamics of **3** are slower than those of **2** and **4** in ethanol. The most likely explanation is the fact that the methoxy groups of **3** are capable of forming hydrogen bonds with ethanol[13], which leads to an increase in the solvent drag for **3**, thus effectively slowing down the phenyl motions.

Figure 6.12 shows the polarization dependent transient behaviour in ethanol. At the red part of the spectrum, similar behaviour as in cyclohexane was observed. The

depolarization of **3** takes slightly longer than that of **2** and **4**, which is indicative of the slower twist in ethanol as just discussed.

More interestingly, the behaviour at 500 nm is somewhat different when compared to cyclohexane. Clearly, the depolarization of the 500 nm transients for **2** and **4** in ethanol is considerably faster. Confirmation of this observation can again be obtained from analyzing the 450 nm transient. Figure 6.13 shows this transient of **2** in ethanol. While the anisotropy in the first few ps is comparable to that in cyclohexane, the depolarization is already complete in 30 ps or less.

Apparently, rotational diffusion takes place much faster in ethanol. This leads to the conclusion that both solvent polarity and solvent viscosity have a distinct effect on the dynamics of such systems, an effect that also has been observed for the dynamics of *cis*- and *trans*-stilbenes[22, 24].

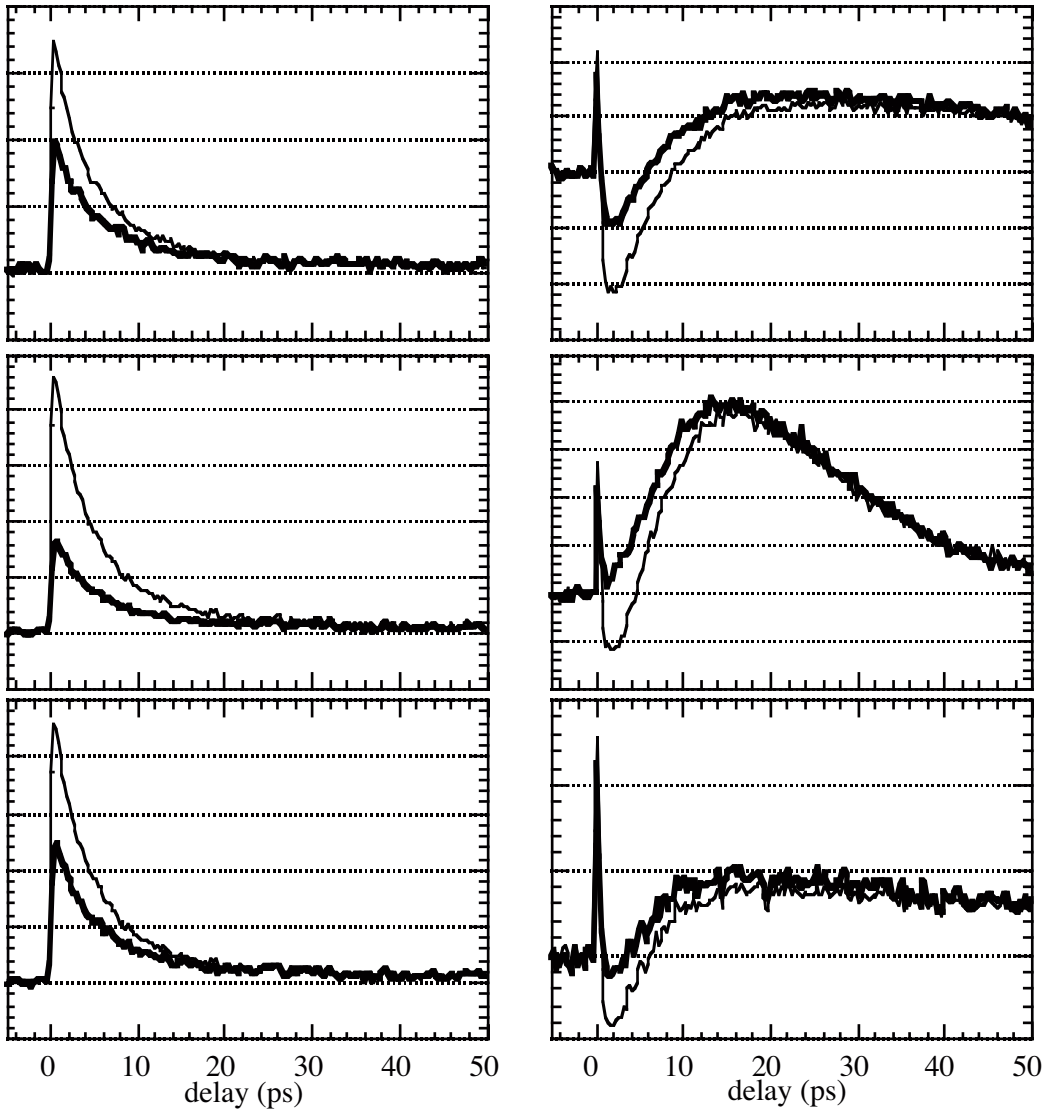

Figure 6.12 600 nm (left panels) and 500 nm (right panels) transients of **2**-**4** (top to bottom) at parallel (thin line) and perpendicular (bold line) pump probe orientation in ethanol.

In figure 6.14 the transients at 500 nm and 600 nm of the substituted TPEs **2**-**4** in cyclohexane and ethanol are compared to those of TPE itself. These two transients are indicative of the behaviour at the blue flank of the spectrum (450-500 nm) and the yellow-red flank of the spectrum (550-650 nm).
The latter transients show little solvent dependence. The shape of the transients is the same in both cyclohexane and ethanol, and the differences in decay dynamics are subtle.

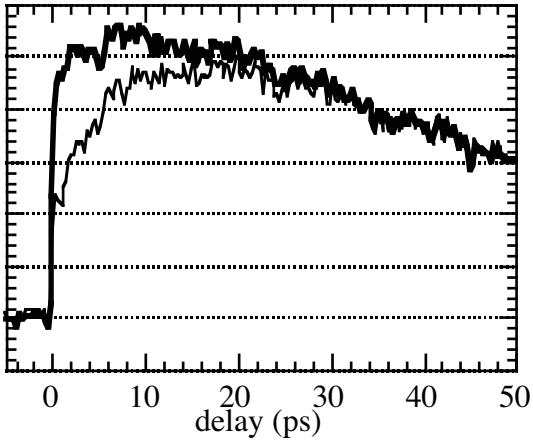

Figure 6.13 Pump probe spectrum (∥: thin line, ⊥: bold line) of **2** at 450 nm in ethanol.

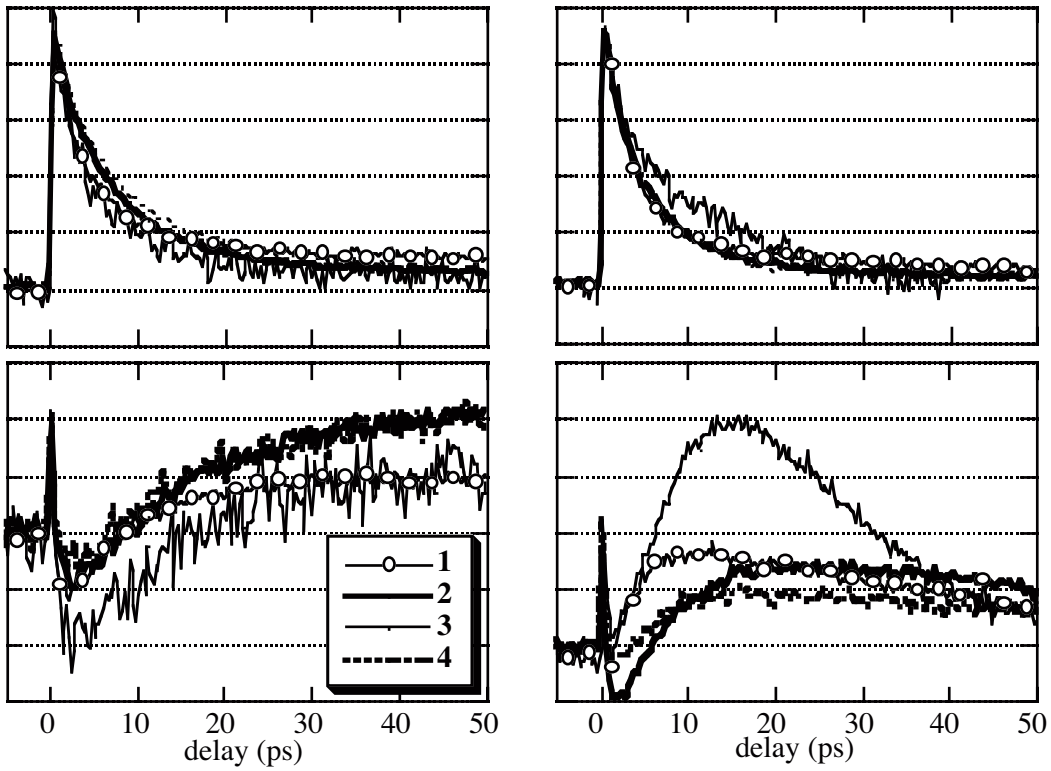

Figure 6.14 Pump probe spectra of **1**-**4** at 600 (∥; top panels) and 500 nm (⊥;bottom panels) in cyclohexane (left panels) and ethanol (right panels).

Apparently, the central bond twisting dynamics that are held responsible for the decay of the red flank of the spectrum are largely solvent independent.

Larger differences can be detected in the green-blue part of the spectrum. Relevant solvatochromic effects can be observed and even in cyclohexane some differences occur between the different compounds even though the overall behaviour appears the same: after 50 ps all transients have reached some sort of steady state which appears to extend into the nanosecond domain. Compounds **2** and **4** show a more intense long-lived absorption at 500 nm than **1** and **3** in cyclohexane. However, care has to be taken with such observations. Even though the intensity of **3** in comparison to **2** and **4** is much smaller, analysis of the data in figure 6.7, which displays the parallel pump probe polarization orientation at 500 nm in cycohexane, shows no significant difference in intensity between **2**-**4**. Therefore, the depolarization rate appears to play a significant role here as well. This topic will be addressed in more detail when the results of the fitting procedure are being discussed (*vide infra*).

A complicating fact is that these transients have been recorded without quantifying the difference absorption in an absolute way. In both chapter 5 and 6, data are scaled with respect to each other by assuming similar response to the pump pulse. In other words, the intensities of the probe transients around t=0 fs are assumed to be similar for the various transients at mutual wavelength and polarization orientation. Even though not unreasonable, this obviously is a somewhat crude scaling method which can easily introduce errors in the relative transient intensities. As a result, comparison of transients from different measurements has to be handled with care especially when (small) differences in intensities are concerned. It should be emphasized, however, that differences in transient shape and decay dynamics as well as large differences in intensities obviously remain highly relevant for the analysis of molecular dynamics.

The behaviour at 500 nm of **1**-**4** exhibits large differences. The most remarkable observation is the intense absorption of **3** and its rapid decay. A possible explanation may be based on the fact that the methoxy groups are capable of special interactions with ethanol, e.g. the formation of hydrogen bonds with the solvent. This can cause increased stabilization of a charge separated state. The rapid decay in ethanol supports this theory, because a short lifetime is indicative of a narrow gap between excited and ground state potential energy surfaces, implying excited state stabilization[5].

Compounds **1** and **2** behave similarly in the later stages of the measurement, but the build-up of **2** is much slower than that of **1**. Finally, the absorption of **4** is surprisingly weak, even though its dynamics appear to roughly resemble those of **1**-**2**. At this point it is interesting to compare the behaviour of **2** and **4** at the blue part of the spectrum in both cyclohexane and ethanol (figure 6.15).

The overall behaviour of **2** and **4** in terms of lifetimes resembles that of **1** in cyclohexane and ethanol (see chapter 5). However, the intensity of especially the 500 nm transients can be regarded as puzzling. Both **1** and **3** have shown a strong increase of the absorption at 500 nm when the polarity of the solvent is increased, but **2** and **4** do not obey this trend. In fact, the buildup at 500 nm is more intense in cyclohexane for **4**, even though its lifetime is much shorter in ethanol.

This is confirmed by the decay dynamics of the 450 nm transient, which decays more rapidly in ethanol for both **2** and **4**, even though the sample time of 50 ps is almost too

short to observe this in the case of **2**. The differences in absorption intensity between **1**-**4** remain difficult to explain, however.

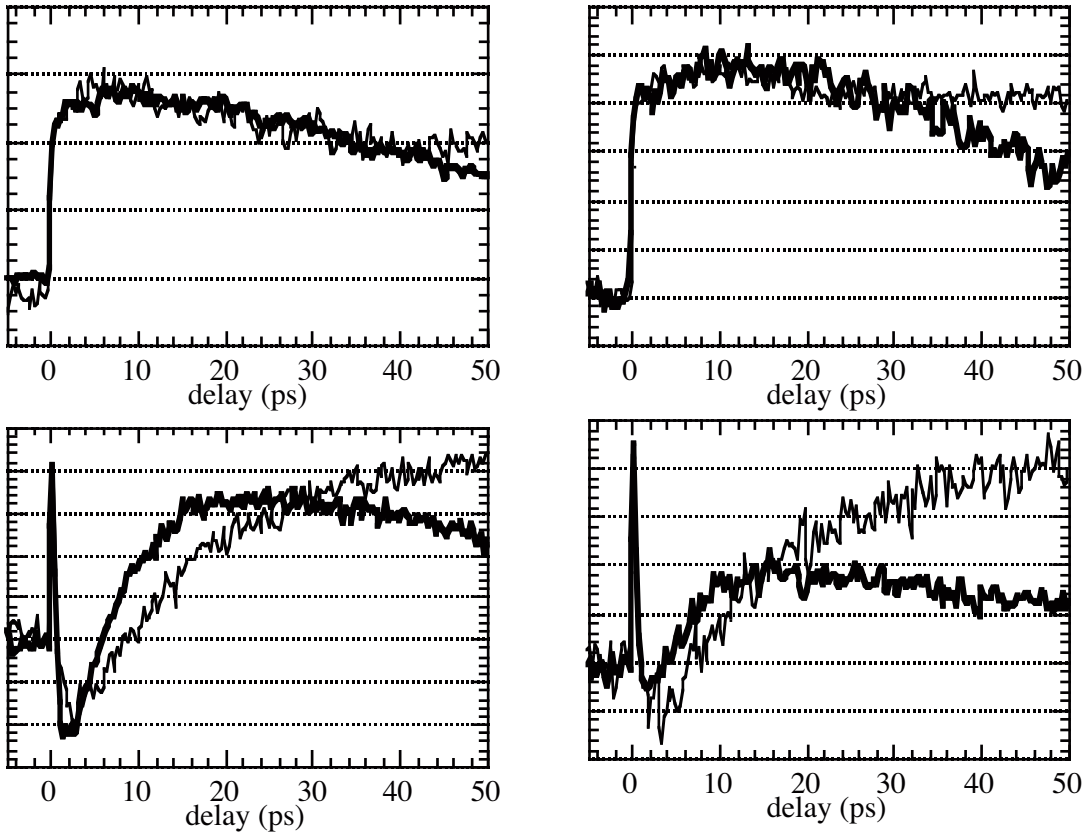

Figure 6.15 Pump probe spectra (⊥) of **2** (left panels) and **4** (right panels) in cyclohexane (thin line) and ethanol (bold line) at 450 nm (top panels) and 500 nm (bottom panels)

In chapter 5, the 500 nm absorption was assigned to the charge separated (CS) state of **1** at the (near) perpendicular geometry. For **3**, this assignment still appears to be valid, but **2** and especially **4** are more difficult to fit in this picture. For instance, this would suggest that for **2** and **4** the CS state is more effectively populated in cyclohexane (see figure 6.15 at 20 ps time scale). It is therefore likely that in this case the scaling of the data to the instantenous response has introduced a margin of error which causes this anomalous difference in intensities.

In order to create more insight in the overall potential energy landscape and the states involved, the global fitting routine as applied to TPE in chapter 5 has been repeated for **2**-**4** (equation 6.1). In this model, A is the Franck-Condon relaxed planar geometry whereas B and C are the perpendicular charge separated and charge resonant states. In the procedure, the 450-650 nm transients from 3-50 ps have been fitted according the kinetic model in equation 6.1, first with assuming K_{bc} and K_{cb} equal to zero. The ∥ oriented signals have been used, except in the case of 450 and 500 nm, for which the transients at both polarization orientations have been included. The first 3 ps have been removed from the fit to exclude the influence of ultrafast dynamics (see section 6.2.1) and vibrational cooling from the data. In cases where the fit to this model proved unsatisfactory, K_{bc} and

K_{cb} were included in the fit. The quality of the fits of **2**-**4** proved to be similar to those of **1** presented in chapter 5. The results are shown in table 6.1.

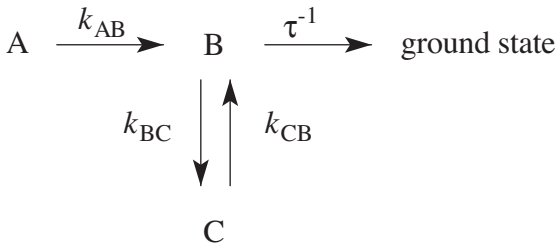

(6.1)

	k_{AB} (ps^{-1})	k_{BC} (ps^{-1})	k_{CB} (ps^{-1})	τ (ps)
cyclohexane				
1	0.46	0.042	0.082	$>10^3$
2	0.25	0.087	--	$>10^3$ a)
3	0.21	0.045	0.060	$>10^3$ a)
4	0.27	0.078	--	$>10^3$ a)
ethanol				
1	0.32			60
2	0.14			70
3	0.10			16
4	0.18			60

Table 6.1 Kinetic parameters for the dynamics of the excited state of **1**-**4**
a) all estimated to be similar to that of **1**

With regard to the twisting from the Franck Condon relaxed excited state to the twisted geometry (i.e. A→B), the fitted data clearly show the increase of solvent drag by the substituents as indicated by the significantly smaller values ofk_{AB} for **2**-**4** with respect to **1**. Intriguingly, the faster central bond rotation of **3** in cyclohexane in comparison to **2** and **4** as suggested by the transients at the red part of the spectrum (as depicted in figure 6.8), is not reproduced by the fit results. No definite explanation for this discrepancy can be provided even though the electronic nature of the methoxy groups must be connected to it. It is likely that the rotation of these groups is seriously hampered in ethanol as a result of the hydrogen bonding which can explain why the depolarization of the red part of the spectrum is in better agreement with the estimated k_{AB}.

The most remarkable finding is that for **2** and **4** in cyclohexane quite excellent fits could be obtained without including k_{CB}.This suggests a three state system for **2** and **4**, which shifts towards the third state without effective repopulation of the second one. This can explain the more intense 'perpendicular' absorption at 500 nm of **2** and **4**, an absorption assigned to the CS state in the case of **1**.

Even though the difference in 500 nm absorption intensity of **4** has already been discussed in terms of transient scaling, it still remains that some dramatic differences in intensity occur especially at the 500 nm transient in ethanol which cannot be explained this way. These remarkable differences in intensity can indicate that the oscillator strength of

the transition is sensitive to a combination of substituent and solvent effects which complicates comparisons between transients in different solvents.

Another possibility is that the λ_{max} of the absorption assigned to the twisted geometry shows solvatochromic behaviour. If, for instance, electron donating substituents cause a red shift whereas electron withdrawing substituents cause a blue shift in polar solvents, the behaviour at 500 nm in ethanol can also be easily explained. In that case, the absorption maximum of **4** will be shifted towards 450 nm. The transient at this wavelength provides hardly any evidence of twisting, as shown in both this as well as the previous chapter. So if the latter assumption is correct, it is impossible to establish an accurate estimate of the quantum yield of the CS state in compounds with electron withdrawing substituents on the basis of this data. This would imply that the weaker intensity of the 500 nm transient of **4** in ethanol is relevant. Unfortunately, at this point no definite evidence supporting either of the two theories is present and, for instance, more extensive DRF studies[25] extending those presented in chapter 4, can be helpful in providing answers to these questions.

The fits clearly show solvatochroic behaviour on the excitated state features. Many lifetimes in nonpolar solvents appears to extend into the nanosecond domain, whereas in ethanol lifetimes are limited to several tens of picoseconds. In cyclohexane, **2** and **4** appear to exhibit more pronounced CS behaviour than **1** and **3** on the basis of the 500 nm transient behaviour, as indicated by the global fits. This seems to indicate that both solvent as well as substituent effects can be the driving force behind the required symmetry breaking in the formation of long-lived CS intermediates. This cannot be fully explained on the basis of the work presented in this and previous chapters, which underlines the complexity of the phenomenon studied here.

In polar solvents like ethanol, the charge separation process appears to be less governed by subtle intramolecular effects. The interaction with the solvent governs this process completely. Especially the short lifetime of **3** indicates additional solvent stabilization of the CS state. This has been attributed to the role of hydrogen bonding between the ethanol acidic proton and the methoxy oxygens of **3**. The other investigated compounds all exhibit CS state lifetimes of 60-70 ps, which supports the theory that solvent rather than the substituent effects govern the electronic processes involved here.

6.3 Summary and Conclusion

In this chapter, time-resolved dual colour femtosecond pump probe studies of **2**-**4** in cyclohexane and ethanol have been presented. It has been shown that the dynamics at the first 2 ps are solvent independent and very similar to that of **1**, even though the elongation of the central bond appears to be slowed down a bit by the introduction of *para*-substituents. These substituents were shown to have a negligible influence on the frequency of the vibrational coherence observed at the 650 nm transient. The recording of the 450 nm probe transient revealed oscillations with the same frequency as those observed at 650 nm, but with the prefect counterphase. This is indicative of wave packet dynamics in a bound potential.

At longer timescales, explicit solvatochromic effects have been observed.

First of all, it has been established that rotation around the central olefenic bond as monitored at the red part of the spectrum, is mainly governed by solvent viscocity. In addition, it has been demonstrated by means of fitting the data to a kinetic model, that the introduction of substituents increase the solvent drag of the phenyl groups leading to a slower central bond twist in comparison to **1**. In the case of **3** this effect has been amplified in ethanol, due to the possible formation of hydrogen bonds with the solvent which introduces additional drag.

The separate detection of probe signals at both parallel and perpendicular orientation relative to the pump polarization has revealed that solvent polarity plays a significant role in the rotational diffusion rate for **2**-**4**. In ethanol, this process takes place much faster than in cyclohexane. It is likely that the polar solvent molecules induce local out-of-plane dipole moments at the (*para*-substituted-)TPEs, which accelerate the reduction of the initial polarization anisotropy. Furthermore, the difference in the depolarization rates at the red and blue flanks of the spectrum has demonstrated the observation of two different depolarization processes: the rotation of the central bond as well as the motion of the complete molecule in the solvent. The most remarkable solvent dependent differences have been observed at the 500 nm transient (⊥), which has been assigned to the CS state of such compounds in chapter 5. In cyclohexane, these transients exhibit lifetimes extending into the nanosecond domain in the case of **1**-**4**. However, the transients of **2** and **4** are more intense than those of **1** and **3**, indicative of a more effective CS state formation in the case of the former two compounds if this state can be held solely responsible for the spectral features of this transient. This is supported by the outcome of the fitting routine, which suggested an equilibrium between two states at the perpendicular geometry for **1** and **3** in this solvent, whereas this equilibrium almost completely shifted to one state in the case of **2** and **4**. Apparently, the *p*-substituents have a distinct influence on the charge separation process, even though no direct correlation with the electronic nature of the subtituents seems to be present. In order to be able to establish such a correlation, a more extensive study including a larger number of *p*-substituted TPE analogues is required. It can be concluded though that both intramolecular and intermolecular (i.e. the solvent) symmetry lowering effects play an important role in the formation of charge separated states.

In ethanol, the lifetimes τ of the probed (*p*-)TPE excited states are drastically shortened in comparison to cyclohexane, indicative of the more effective CS formation and stabilization for **1**-**4**. This appeared to be especially the case for **3** (τ=15 ps), whereas the other three compounds exhibited lifetimes of approximately 60 ps. Possibly, formation of hydrogen bonds plays an important role in the stabilization of the CS state. Another remarkable finding has been the strong differences in absorption intensity at 500 nm in ethanol. On the basis of the results of the global fitting procedure it could not be established whether or not the CS state was less effectively populated in cases where the 500 nm absorption was weak. It is possible that the λ_{max} of the CS excitation probed here is subject to solvatochromic influences and that this is the main reason for the observed differences in intensity at 500 nm.

6.4 References

1. B.I. Greene, Chem. Phys. Lett., **79**, 51-53 (1981).
2. P.F. Barbara, S.D. Rand and P.M. Rentzepis, J. Am. Chem. Soc., **103**, 2156-2162 (1981).
3. C.L. Schilling and E.F. Hilinski, J. Am. Chem. Soc., **110**, 2296-2298 (1988).
4. J. Ma and M.B. Zimmt, J. Am. Chem. Soc., **114**, 9723-9724 (1992).
5. J. Morais, J. Ma and M.B. Zimmt, J. Phys. Chem., **95**, 3885-3889 (1991).
6. W. Schuddeboom, S.A. Jonker, J.M. Warman, M.P. de Haas, M.J.W. Vermeulen, W.F. Jager, B. de Lange, B.L. Feringa and R.W. Fessenden, J. Am. Chem. Soc., **115**, 3286-3290 (1993).
7. Y-P. Sun and C.E. Bunker, J. Am. Chem. Soc., **116**, 2430-2433 (1994).
8. T. Tahara and H. Hamaguchi, Chem. Phys. Lett., **217**, 369-374 (1994).
9. J. Ma, G. Bhaskar Dutt, D.H. Waldeck and M.B. Zimmt, J. Am. Chem. Soc, **116**, 10619-10629 (1994).
10. E. Lenderink, K. Duppen and D.A. Wiersma, J. Phys. Chem., **99**, 8972-8977 (1995).
11. R.W.J. Zijlstra, P. Th. van Duijnen, B.L. Feringa, T. Steffen, K. Duppen and D.A. Wiersma, J. Phys. Chem. A, **101**, 9828-9836 (1997).
12. G.R. Fleming, *Chemical Applications of Ultrafast Spectroscopy*, Oxford University Press, New York, 1986.
13. S.H. Pine, *Organic Chemistry*, McGraw-Hill Book Company, New York, 1987.
14. R.C. Weast, M.J. Astle and W.H. Beyer, *Handbook of Chemistry and Physics*, CRC Press Inc., Boca Raton, Fl., USA, 1985-1986.
15. C.J. Bardeen, Q. Wang and C.V. Shank, Phys. Rev. Lett., **75**, 3410-3413 (1995).
16. Z. Rappoport and S.E. Biali, Acc. Chem. Res., **30**, 307-314 (1997).
17. M. Dantus, R.M. Bowman, M. Gruebele and A.H. Zewail, J. Chem. Phys., **91**, 7437-7450 (1989).
18. U. Banin, A. Waldman and S. Ruhman, J. Chem. Phys., **96**, 2417-2419 (1992).
19. U. Banin and S. Ruhman, J. Chem. Phys., **98**, 4391-4403 (1993).
20. Q. Wang, R.W. Schoenlein, L.A. Peteanu, R.A. Mathies and C.V. Shank, Science, **266**, 422-424 (1994).
21. N.J. Turro, *Modern Molecular Photochemistry*, The Benjamin/Cummings Publishing Company, Inc., Menlo Park, CA, 1978.
22. D.H. Waldeck, Chem. Rev., **91**, 415-436 (1991).
23. C.T. Lin, H.W. Guan, R.K. McCoy and C.W. Spangler, J. Phys. Chem., **93**, 39-43 (1989).
24. R.A. McGill, J.K. Rice, A.P. Baranovski, J.C. Owrutsky, A.H. Lowrey, K.K. Stavrev, T. Tamm and M.C. Zerner, Int. J. Quant. Chem. Symp., **30**, 383-394 (1996).
25. P. Th. van Duijnen, A.H. Juffer and H.P. Dijkman, J. Mol. Struct. (THEOCHEM), **260**, 195-205 (1992).